Large Slip of Aqueous Liquid Flow over a Nanoengineered Superhydrophobic Surface

Chang-Hwan Choi* and Chang-Jin Kim

Mechanical and Aerospace Engineering Department, University of California, Los Angeles, California 90095, USA

(Received 14 September 2005; published 16 February 2006)

While many recent studies have confirmed the existence of liquid slip over certain solid surfaces, there has not been a deliberate effort to design and fabricate a surface that would maximize the slip under practical conditions. Here, we have engineered a nanostructured superhydrophobic surface that minimizes the liquid-solid contact area so that the liquid flows predominantly over a layer of air. Measured through a cone-and-plate rheometer system, the surface has demonstrated dramatic slip effects: a slip length of $\sim 20\ \mu$m for water flow and $\sim 50\ \mu$m for 30 wt % glycerin. The essential geometrical characteristics lie with the nanoposts populated on the surface: tall and slender (i.e., needlelike) profile and submicron periodicity (i.e., pitch).

DOI: 10.1103/PhysRevLett.96.066001 PACS numbers: 83.50.Rp, 47.45.Gx, 68.08.Bc, 81.40.Pq

To assume zero flow velocity at a wall, i.e., a "no-slip" boundary condition, is a fundamental element in analyzing continuum fluid flow [1]. However, several molecular dynamics simulations have shown that the slip can be conditioned through changes in fluid-surface interactions [2,3]. Because the effect of deviation from the traditional no-slip assumption becomes pronounced when the scale of interest goes down to microns and below, there has been a growing interest in characterizing the slip over various surfaces, especially in liquid flow [4]. While a few reports have addressed the slip over hydrophilic surfaces [5], many have reported that certain hydrophobic surfaces allow noticeable slip, with slip lengths in the range of 30 nm to 1 μm, theoretically [6], experimentally [7–17], and numerically [18]. Several reasons have been proposed for the slip over hydrophobic surfaces: molecular slip [6], small dipole moment of polar liquids [17], and gas gaps or nanobubbles at the solid-liquid interface [8,16,19]. In particular, rough hydrophobic surfaces, so-called "superhydrophobic" surfaces [20] have been shown to generate an "effective" liquid slip because of the air trapped between the surface structures [21–23].

Despite the studies, there has not been a deliberate effort to *design* a low-friction surface of engineering significance: a large slip effect for pressurized flows. The fine grooves (i.e., cracks) in the rough surface in [22] constitute only a small fraction of the surface and the rest of the surface is also rough, making it difficult to isolate the effect of trapped air. Although the lithographically patterned hydrophobic mesa structures in [23] may be a convenient way to demonstrate large slip effects, their pitches of many microns would limit the surface function only under small liquid pressures (<0.05 atm). Our goal, extended from our previous report for droplet flows [24], is to fabricate a solid surface full of tall and sharp nanoposts with a submicron pitch, which would accommodate many pressurized (~ 1 atm) flows, and demonstrate a large slip effect for continuous flows.

Let us imagine Couette flow in which an air layer separates liquid from a wall by the sharp tips of the hydrophobic posts, as shown in Fig. 1. Riding mainly over air, the liquid is expected to flow over the solid surface experiencing little friction. If one neglects the post structures (as an ideal case), a slip length δ due to the pure air layer of thickness b can be represented by

$$\delta = b(\mu_l/\mu_a - 1), \tag{1}$$

where μ_l and μ_a are the viscosities of liquid and air, respectively [10]. A large effective slip is expected due to the sizable viscosity difference between liquid and air, larger with a thicker air layer. For example, if the liquid is water and the air is 1 μm thick, the slip length δ would be $\sim 54\ \mu$m, disregarding the deviation from continuum at this scale to simplify the discussion.

For the design of the surface structures, consider conical posts of height b and cone angle 2α as shown in Fig. 1. The posts are assumed to form a square array with a pitch d. The meniscus is assumed to be of a spherical shape with

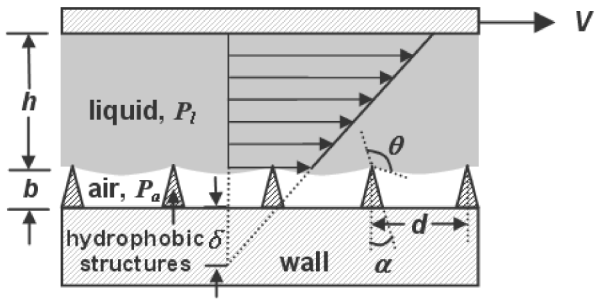

FIG. 1. Concept of large effective slip by a nanoengineered superhydrophobic surface in Couette flow. Liquid sits on hydrophobic structures by surface tension. The majority of the liquid boundary is with air, where shear stress is much smaller. The hydrophobic structures need to be relatively tall and populated in submicron scale to sustain the liquid levitation and to produce the effective slip over air under realistic conditions (i.e., pressure ranging up to 1 atm).

contact angle θ (or advancing contact angle θ_A when the liquid pressure increases) on the side surfaces of the posts, balancing with the liquid pressure. The posts need to be tall enough so that the meniscus does not touch the bottom surface between posts [25]. The posts also need to be populated densely enough, i.e., the pitch should be small enough, so that the surface tension of the warped meniscus withstands the pressure in the liquid. By a simple geometrical calculation and the Laplace-Young equation, the post height b and the interpost pitch d to hold up the liquid meniscus against the pressure of liquid over air ($\Delta P = P_l - P_a$) can be obtained as

$$b > \frac{1 - \sin(\theta_A - \alpha)}{\sqrt{2}|\cos(\theta_A - \alpha)|} d, \qquad d < 2\sqrt{2}\sigma \frac{|\cos(\theta_A - \alpha)|}{\Delta P}, \tag{2}$$

where σ is the surface tension of the liquid-air interface. For example, if the liquid is water ($\sigma = 0.0727$ N/m at 20 °C), ΔP is 0.1 MPa (~1 atm), and ($\theta_A - \alpha$) is 120° [26], the pitch d should be less than ~1 μm, and the post height b should be larger than ~0.2 μm. It is further desired to make the posts sharp at the tip so that the liquid-solid contact area is minimized and slender in shape so that the contribution of air is maximized.

Considering the design requirements above, needle structures with 1–2 μm height and 0.5–1 μm pitch were fabricated on a silicon wafer by the black silicon method [24], generating the surface we call ''nanoturf'' (Fig. 2). The fracture stress of silicon is very high ($\cong 2.2 \times 10^9$ Pa) so that the slender nanoscale structures assure enough robustness against external stresses induced even by extreme flows. The surface was treated to be either hydrophilic by O_2 plasma or hydrophobic by spin coating of Teflon® AF (DuPont). The Teflon thickness was estimated to be 10–20 nm, as determined from cross-sectional scanning electron microscope (SEM) images of the nanoturf structures taken before and after the coating, which is consistent with an ellipsometer measurement on a smooth surface. As references, both hydrophilic and hydrophobic smooth surfaces were also prepared directly on silicon. A surface roughness of ~3 Å was measured for the hydrophilic and ~6 Å for the hydrophobic surface by atomic force microscope. The contact angles of water were measured by a goniometer to be ~10° on the hydrophilic smooth surface, ~0° on the hydrophilic nanoturf, ~120° on the hydrophobic smooth surface, and over 175° on the hydrophobic nanoturf.

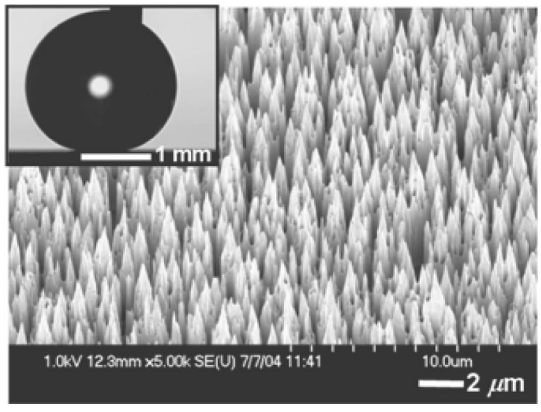

FIG. 2. SEM image of a nanoturf surface made by the black silicon method [24]. The inset shows the apparent contact angle of water droplet (i.e., ~180°) on the nanoturf surface after the hydrophobic coating with Teflon.

The slip length was obtained through torque measurement with a commercial rheometer (AR 2000, TA Instruments, New Castle, Delaware, USA), whose operational torque range is between 0.1 μN m and 200 mN m with angular velocity between 10^{-8} and 300 rad/s. A cone-and-plate arrangement, the most popular geometry because of the uniform shear rate over a sample, was used (Fig. 3). In the present experiment, a stainless steel cone of 60 mm in diameter, 2° in cone angle, and 53 μm in truncation is used. For the bottom plate, the prepared test substrates with the four different surface conditions (i.e., hydrophilic smooth, hydrophobic smooth, hydrophilic nanoturf, and hydrophobic nanoturf) are placed over a rheometer stage with temperature set by a Peltier plate at 20 ± 0.1 °C. The test liquids are deionized water and the aqueous solution of glycerin at 30 wt% concentration. They are dispensed between the cone and the test substrate by pipetting ~1.98 mL, which is the volume for a correct filling.

When a cone of radius R and very small cone angle θ_0 rotates at angular velocity Ω, the governing equation of the Couette flow with a slip on the substrate can be represented by

$$\frac{\partial \tau_{\theta\phi}}{\partial \theta} + 2\tau_{\theta\phi}\cot\theta = 0, \tag{3}$$

$$\nu_\theta(\pi/2, r) = \nu_s, \qquad \nu_\theta(\pi/2 - \theta_0, r) = \Omega r, \tag{4}$$

where $\tau_{\theta\phi}$ is the shear stress in the ϕ direction and slip velocity ν_s is applied at the substrate wall. If we use Navier's hypothesis about the wall slip (i.e., a slip velocity is proportional to the shear rate at a wall) and the wall shear stress $\tau_{\theta\phi}$ is expanded into a Taylor series as a function of $\delta/(r\theta_0)$, the torque M on the rotating cone can be calculated as

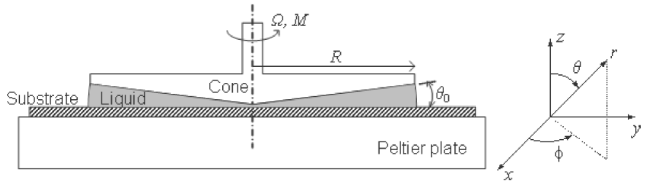

FIG. 3. Schematic drawing of a cone-and-plate rheometer, showing the geometric parameters and the reference frames for the analysis of the Couette flow within it.

$$M = \int_0^R 2\pi r^2 \tau_{\theta\phi} dr = \frac{2\pi}{3} \frac{\mu \Omega R^3}{\theta_0} \left(1 - \frac{3\delta}{2R\theta_0} + \frac{3\delta^2}{R^2\theta_0^2}\right), \quad (5)$$

where the viscosity μ of the test liquid is assumed to be constant, and terms of $\delta/(R\theta_0)$ higher than the second order are discarded for simplification. Derived from the torque measurement for each sample, the degree of slip is quantified by slip length δ, which can be calculated as

$$\delta = \frac{R\theta_0}{4} \left(1 - \sqrt{\frac{8\theta_0}{\pi \Omega R^3} \frac{M}{\mu} - \frac{13}{3}}\right), \quad (6)$$

where the viscosity μ of the test liquid is measured from a capillary viscometer (i.e., a glass capillary tube) and confirmed to coincide with the known fluid properties: $\mu_w = 1.0 \times 10^{-3}$ Pa s for water and $\mu_g = 2.5 \times 10^{-3}$ Pa s for 30 wt% glycerin at 20 °C. The torque applied to the rotating cone was measured over various shear rates. At each shear rate, the average torque over a few minutes was recorded after reaching a steady state with less than 3% deviation. Each sample was tested several times to ensure reproducibility.

Figure 4 shows the collection of the slip lengths for all four surfaces in the flow of water and the 30 wt % glycerin. The data were obtained within the reliable shear rate range, e.g., free of secondary flow, for the corresponding liquid. As postulated earlier, the hydrophobic nanoturf surface demonstrates a dramatic slip effect of ~20 μm in water flow and ~50 μm in 30 wt % glycerin, while the other three surfaces do not show discernible slip in this experiment. The indiscernible slips, however, are not to contradict the reported slip over a smooth hydrophobic surface [6–18] and even over a smooth or rough hydrophilic surface [5]. The standard deviation of the slip length data in our experiment is ~3 μm, simply too large for all other surfaces whose slip lengths are typically smaller than 1 μm. Instead, the key here is that our nanoengineered surface has a much larger slip (i.e., at least 2 orders of magnitude higher) than what we may expect from all other surfaces. Along with the compatibility with pressurized flows, this level of large slip effect is useful for engineering purposes.

Note that the results of hydrophobic nanoturf show that the slip length for 30 wt % glycerin is ~2.5 times that for water, consistent with the viscosity ratio of ~2.5. In reference to Eq. (1), which states that the slip length should be proportional to the viscosity of the test liquid, the result supports the reliability of the measurements and suggests that a more pronounced slip effect (i.e., larger slip length) is expected with a more viscous liquid on the hydrophobic nanoturf surface. According to Eq. (1), the hydrophobic nanoturf, whose posts are 1–2 μm thick, has produced the slip effect equivalent to a ~0.4 μm thick pure air layer. This is a reasonable result, considering the relative air fraction of the nanoturf (estimated ~60% from Fig. 2)

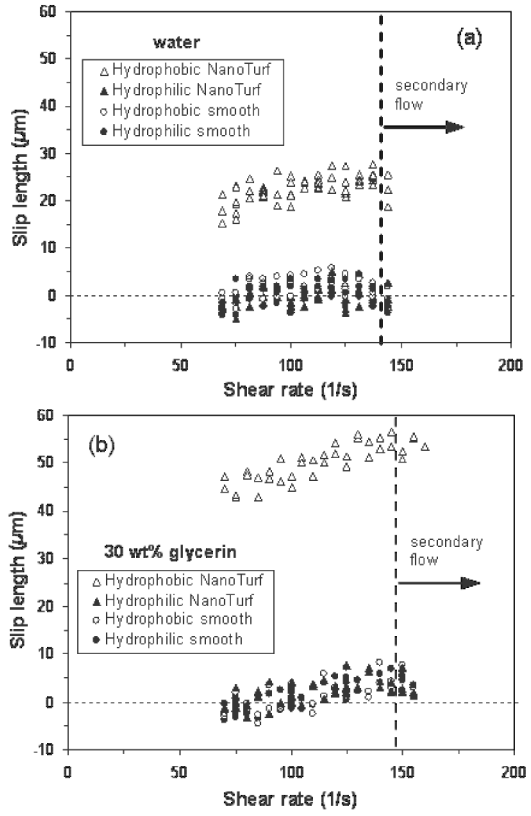

FIG. 4. Experimental results for slip length. Hydrophobic nanoturf (△) shows dramatic slip for both (a) water (~20 μm) and (b) glycerin (~50 μm), while all other surfaces show slip comparable to measurement uncertainties. The superhydrophobicity of the nanoturf surface was preserved throughout the experiment with the slip length undiminished over time, suggesting that the large effective slip by the air trapped on the hydrophobic nanoturf surface is not temporary. The secondary flow was verified experimentally by observing the torque versus shear rate data [27]. As the secondary flow became present, the torque increased not linearly but exponentially with shear rate, which was reflected in the results as the onset of the slip length reduction. Although the data were not shown here, the torque over the hydrophobic nanoturf was much smaller than the other surfaces even in the secondary flow regime, suggesting that the drag reduction by the large effective slip is still valid in the unstable flow regime.

and the nonuniform flow field, which constantly develops along the repeated solid tips and air interfaces.

Although shear-rate-dependent slip has been reported in several studies [2,8,9,13,15], the range of shear rates covered in the present experiment is too narrow to confirm the shear-rate-dependent slip. Instead, the apparent increase of slip length with shear rate shown in Fig. 4 is considered to be caused by an experimental artifact, such as viscous heating [27]. Although the temperature of the sample is controlled to be constant by the Peltier plate, a slight change in temperature of the test liquid by viscous heating is expected, especially at high shear rates, affecting the viscosity of the test liquid. For example, a 0.1 °C increase

of temperature from the set point of 20 °C, which corresponds to the uncertainty level of the Peltier plate, is estimated to generate a ~ 2 μm increase in the slip length result. At the same shear rate, a temperature change by viscous heating will be more pronounced in more viscous liquid glycerin than in water, which is confirmed in Fig. 4(b) where a clearer increase of the slip length with shear rate is shown. The applied pressure to the test liquid by the rotating cone was also monitored by the rheometer system to examine the influence of pressure on the effective slip. Although the pressure slightly decreased with shear rate, the measured pressure was low (i.e., less than 1 kPa) so that the corresponding deformation of the liquid meniscus over the hydrophobic nanoturf structures was estimated to be negligibly small (i.e., less than 1 nm sag down), suggesting that the pressure is not involved in the shear-rate-dependent slip in the current experimental conditions.

The slip effect on the surface entails meaningful drag reduction for various flow conditions. Consider Couette flow, for example, with two parallel plates separated by a gap h. If one of the two surfaces has a slip length δ, the drag reduction can be estimated as

$$\left.\frac{\tau_{\text{slip}}}{\tau_{\text{no-slip}}}\right|_{\text{Couette}} = \frac{1}{1 + (\delta/h)}, \tag{7}$$

where τ_{slip} and $\tau_{\text{no-slip}}$ are the shear stresses at a wall when slip and no-slip boundary conditions are applied, respectively. Large drag reduction can be obtained as the gap between the plates becomes smaller, especially down to the range comparable to the slip length. For example, over 66% or 83% drag reduction is expected for water or 30 wt % glycerin, respectively, at the gap of 10 μm.

The results above suggest that the hydrophobic nanoturf surface engineered in this study can reduce the friction in liquid flow significantly not only for droplets [24] but also in continuous flows in various microscale fluidic problems. It could also be applied to reduce the viscous skin friction in macroscale applications, if the boundary layer thickness of the body in the flow is comparable to the slip length. While this study was performed in the laminar-flow regime with moderate Reynolds number of 10–1000, these results prompt the investigation of the slip effect of the nanoturf in a turbulent flow regime with high Reynolds number as well [28,29], since most macroscale flow extends from laminar to turbulent flow.

This research has been funded by the National Science Foundation NIRT Grant No. 0103562. The authors would like to acknowledge Professor Joonwon Kim for the initial nanoturf sample and Professor Pirouz Kavehpour for his help with the rheometer experiment.

*To whom correspondence should be addressed.
Electronic address: chchoi@ucla.edu

[1] S. Richardson, J. Fluid Mech. **59**, 707 (1973).
[2] P. A. Thompson and S. M. Troian, Nature (London) **389**, 360 (1997).
[3] M. Cieplak, J. Koplik, and J. R. Banavar, Phys. Rev. Lett. **86**, 803 (2001).
[4] S. Granick, Y. Zhu, and H. Lee, Nat. Mater. **2**, 221 (2003).
[5] E. Bonaccurso, M. Kappl, and H.-J. Butt, Phys. Rev. Lett. **88**, 076103 (2002); E. Bonaccurso, H.-J. Butt, and V. S. J. Craig, *ibid.* **90**, 144501 (2003).
[6] T. D. Blake, Colloids Surf. **47**, 135 (1990).
[7] E. Schnell, J. Appl. Phys. **27**, 1149 (1956).
[8] E. Ruckenstrein and P. Rajora, J. Colloid Interface Sci. **96**, 488 (1983).
[9] N. V. Churaev, V. D. Sobolev, and A. N. Somov, J. Colloid Interface Sci. **97**, 574 (1984).
[10] O. I. Vinogradova, Langmuir **11**, 2213 (1995); Int. J. Miner. Process. **56**, 31 (1999).
[11] R. Pit, H. Hervet, and L. Leger, Phys. Rev. Lett. **85**, 980 (2000).
[12] J. Baudry *et al.*, Langmuir **17**, 5232 (2001).
[13] Y. Zhu and S. Granick, Phys. Rev. Lett. **87**, 096105 (2001); **88**, 106102 (2002).
[14] C. Cottin-Bizonne *et al.*, Eur. Phys. J. E **9**, 47 (2002).
[15] C.-H. Choi, K. J. A. Westin, and K. S. Breuer, Phys. Fluids **15**, 2897 (2003).
[16] D. Tretheway and C. Meinhart, Phys. Fluids **14**, L9 (2002); **16**, 1509 (2004).
[17] J.-H. J. Cho, B. M. Law, and F. Rieutord, Phys. Rev. Lett. **92**, 166102 (2004).
[18] J.-L. Barrat and L. Bocquet, Phys. Rev. Lett. **82**, 4671 (1999).
[19] P. G. de Gennes, Langmuir **18**, 3413 (2002); E. Lauga and H. A. Stone, J. Fluid Mech. **489**, 55 (2003).
[20] R. Blossey, Nat. Mater. **2**, 301 (2003).
[21] C. Cottin-Bizonne *et al.*, Nat. Mater. **2**, 237 (2003).
[22] K. Watanabe, Y. Udagawa, and H. Udagawa, J. Fluid Mech. **381**, 225 (1999); K. Watanabe *et al.*, AIChE J. **49**, 1956 (2003).
[23] J. Ou, B. Perot, and J. P. Rothstein, Phys. Fluids **16**, 4635 (2004); J. Ou and J. P. Rothstein, *ibid.* **17**, 103606 (2005).
[24] J. Kim and C.-J. Kim, in *Proceedings of the 15th IEEE International Conference on Micro Electro Mechanical Systems* (IEEE, Piscataway, 2002), p. 479.
[25] We speculate that the hydrophobic surfaces with molecular or nanometer scale roughness in Refs. [11,13] did not show slip because the surface features in the molecular or nanometer scale roughness were not tall enough to hold up the liquid meniscus and to contain air, which would produce the effective slip.
[26] Although the ΔP pertinent to this study (i.e., Couette flow in rheometer system) was relatively small (i.e., less than 1 kPa), the post structures were designed to be applicable even under a pressurized condition up to 1 atm. For the present experiment, the advancing contact angles θ_A of water and 30 wt % glycerin over the Teflon-coated hydrophobic surface are both $\sim 130°$.
[27] K. Walters, *Rheometry* (Chapman and Hall, London, 1975).
[28] L. Sirovich and S. Karlsson, Nature (London) **388**, 753 (1997).
[29] T. Min and J. Kim, Phys. Fluids **16**, L55 (2004).